Electrochemistry Communications 155 (2023) 107581

Contents lists available at ScienceDirect

Electrochemistry Communications

journal homepage: www.elsevier.com/locate/elecom

Ion-exchange enabled new intercalation Li metal fluorides

Yichao Wang [1], Xianguang Miao [1], Yitong Li [1], Hwanyeol Park, Yang Lu, Xin Li [*]

John A. Paulson School of Engineering and Applied Sciences, Harvard University, Cambridge, MA 02138, USA

ARTICLE INFO

Keywords:
Li ion cathode
Intercalation
Fluoride
Ion exchange

ABSTRACT

Most metal fluorides-based Li ion battery cathodes suffer from large voltage polarization, volume change, slow rate, and capacity loss in battery cycling due to Li conversion reactions. Here we report a new type of intercalation Li metal fluorides obtained from Li/Na ion exchange of Na-intercalation compounds. The strategy enables a broad chemical design space of new intercalation compounds through the coupling of chemical and electrochemical synthesis pathways at drastically different temperatures. Both voltage plateau and cyclability can be tuned by composition control from chemical synthesis. Our Na/Li ion-exchange strategy thus opens the door to a family of intercalation Li metal fluorides that were not accessible previously due to conversion reactions of such compounds from direct chemical synthesis.

1. Introduction

Intercalation type of lithium layered transition metal oxide ($LiTMO_2$) with high energy density and cycling stability is widely used in batteries such as electric vehicles. However, due to the high Ni and Co compositions, the price of $LiTMO_2$ batteries will increase substantially with upcoming Ni and Co supply crisis [1], which motivates the search of new cathode materials. Metal fluorides [2–7] are promising active materials due to the high electronegativity of fluorine that provides the possibility for high voltage. However, most of the metal fluorides suffer from large voltage polarization, volume change, slow rate, and capacity loss due to Li conversion reactions rather than the desired Li intercalation ones [8].

Here we report a new type of intercalation Li metal fluoride obtained from Li/Na ion exchange of Na-intercalation $Na_2TM_2F_7$ [9–14], which computationally could reach 6 V [9] when de-intercalating more than one Na from the formula. $Na_2Fe_2F_7$ (Fe227), $Na_2Mg_{0.5}Fe_{1.5}F_7$ (MgFe227), and $Na_2Mg_{0.2}Ni_{0.1}Ti_{0.1}Fe_{0.8}V_{0.8}F_7$ (FeVMNT) are successfully synthesized and can stably cycle in a Li half-cell with Li ion liquid electrolyte and Li metal anode. Fe227 can cycle at 1C for 100 cycles with peak capacity of 124 mAh/g. We also use Fe227 to demonstrate the chemical ion exchange ability. MgFe227 can cycle at 2C for 400 cycles with peak capacity of 105 mAh/g. FeVMNT shows a high voltage plateau at around 4 V. Our result shows the opportunity to utilize the broad chemical space for the design of new intercalation type of Li metal fluoride.

2. Experimental

Materials synthesis: $Na_2Fe_2F_7$, $Na_2Mg_{0.5}Fe_{1.5}F_7$ and $Na_2Mg_{0.2}Ni_{0.1}Ti_{0.1}Fe_{0.8}V_{0.8}F_7$ were synthesized by solid-state reactions. NaF (Alfa, 99 %), FeF_2 (Aldrich, 98 %), FeF_3 (Alfa, 97 %), MgF_2 (Aldrich, 99 %), TiF_3 (Aldrich), NiF_2 (Aldrich), VF_3 (Alfa, 98 %) were mixed in appropriate ratios, sealed in a silicon nitride jar in an Ar-filled glove box and ground by high-energy ball milling at 400 rpm for 12 h. The mixture was then pressed into pellets and calcined in a tube furnace in argon gas flow. The temperature increased at 5 °C min^{-1} to 650 °C for $Na_2Fe_2F_7$, 550 °C for $Na_2Mg_{0.5}Fe_{1.5}F_7$, and 500 °C for $Na_2Mg_{0.2}Ni_{0.1}Ti_{0.1}Fe_{0.8}V_{0.8}F_7$, kept constant for 30 min and naturally cooled down in the furnace.

Battery test: $Na_2Fe_2F_7$, $Na_2Mg_{0.5}Fe_{1.5}F_7$, and $Na_2Mg_{0.2}Ni_{0.1}Ti_{0.1}Fe_{0.8}V_{0.8}F_7$ were mixed with carbon black and carbon nanotube at 70:19:1 wt ratio and ball-milled in Ar filled and airtight silicon nitride jar at 150 rpm for 12 h. The mixture is then mixed with PTFE binder at 95:5 wt ratio to make a dry cathode film (2 mg/cm^2). For Lithium half cell, Li metal was used as a negative electrode. 1 M $LiPF_6$ in EC/DEC (1:1 v/v, Aldrich) and a glass fiber filter GF/D (Whatman) were used as an electrolyte and a separator, respectively. For Na half cell, Na metal and 1 M $NaPF_6$ in EC/DEC (1:1) were used. Swagelok type cells were assembled in an Ar-filled glove box and tested on an LAND battery testing station. Each battery contains ~ 0.5 mg cathode active material and 100 ul electrolyte to dilute the Na ion from intial charge to around 1:50 Na^+ to Li^+ molar ratio in the electrolyte calculated assuming all Na

* Corresponding author.
E-mail address: lixin@seas.harvard.edu (X. Li).
[1] Y.W., X.M. and Y.Li. contributed equally to this paper.

https://doi.org/10.1016/j.elecom.2023.107581
Received 23 August 2023; Received in revised form 6 September 2023; Accepted 13 September 2023
Available online 15 September 2023
1388-2481/© 2023 The Authors. Published by Elsevier B.V. This is an open access article under the CC BY-NC-ND license (http://creativecommons.org/licenses/by-nc-nd/4.0/).

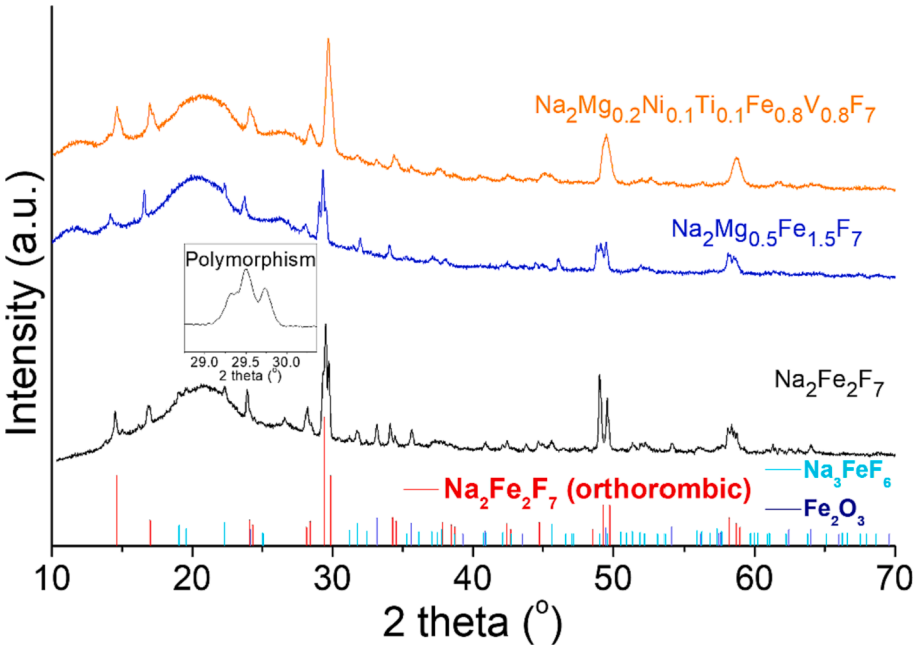

Fig. 1. X-ray Diffraction (XRD) pattern of three different $Na_2TM_2F_7$ compounds of $Na_2Fe_2F_7$ (Fe227), $Na_2Mg_{0.5}Fe_{1.5}F_7$ (MgFe227) and $Na_2Mg_{0.2}Ni_{0.1}Ti_{0.1}Fe_{0.8}V_{0.8}F_7$ (FeVMNT). The inset enlarges the peaks at around 29.5°. The simulated Bragg peaks at bottom label the expected peak positions for orthorhombic $Na_2Fe_2F_7$ main phase and two impurity phases of Na_3FeF_6 and Fe_2O_3, which are minor in the experimental XRD.

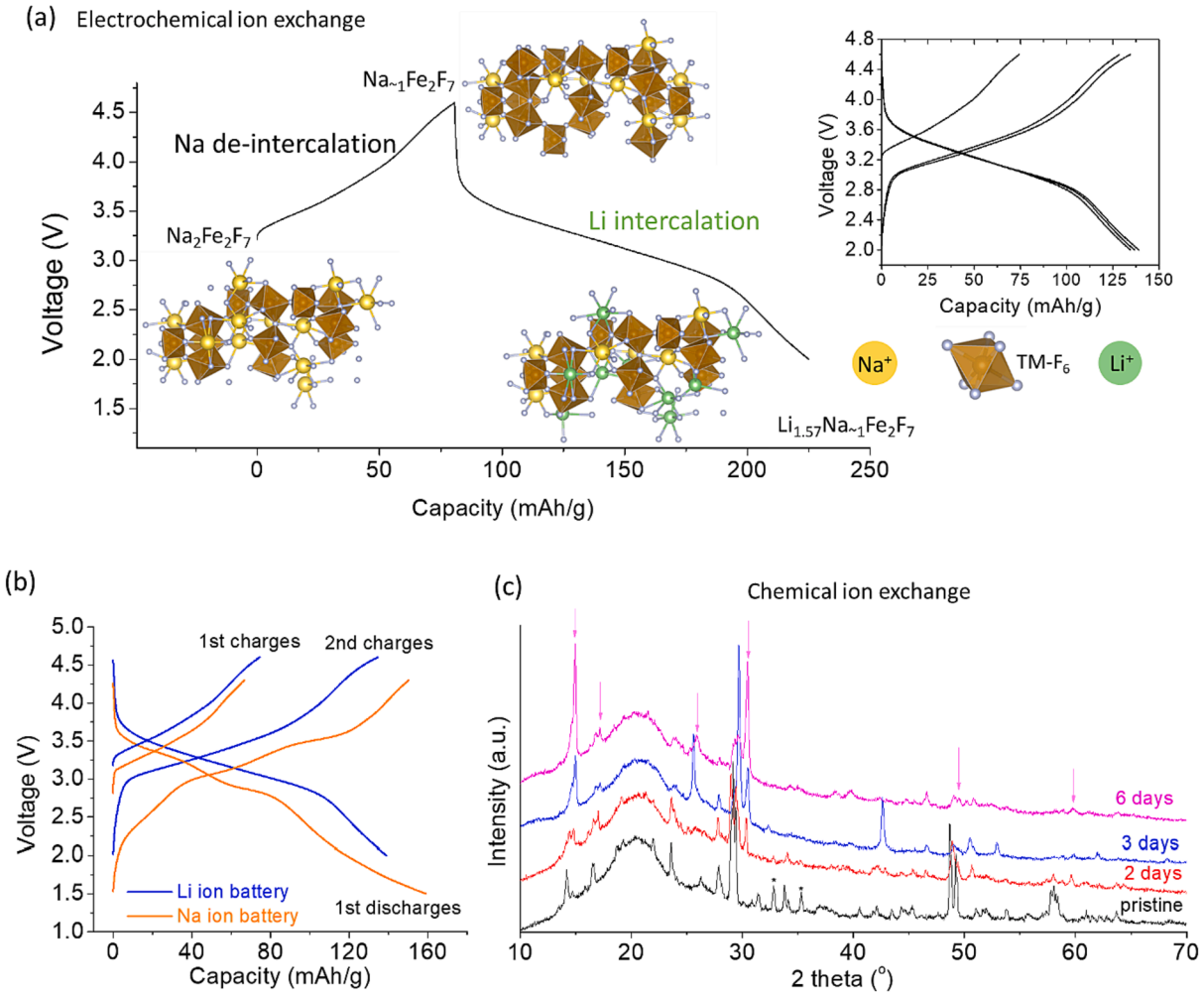

Fig. 2. Electrochemical and chemical Li/Na ion exchange of $Na_2Fe_2F_7$ (Fe227). (a) $Na_2Fe_2F_7$ is directly charged and discharged in $LiPF_6$ electrolyte with Li metal anode ($Na_2Fe_2F_7$|Li). Crystal model illustrates the de-sodiation and lithiation process. The inset shows the first three cycles of the $Na_2Fe_2F_7$|Li half-cell battery. (b) Voltage curve comparison of $Na_2Fe_2F_7$|Li and $Na_2Fe_2F_7$|Na half-cell. (c) Ex situ XRD evolution of chemical ion exchanged $Na_2Fe_2F_7$ by soaking in 5 M LiBr hexanol solution. The star for the pristine pattern labels the Fe_2O_3 impurity.

ion stays in the electrolyte.

X-ray diffraction (XRD): XRD data were obtained using a Rigaku Miniflex 6G. Powder samples were sealed with Kapton film in an argon-filled glovebox before XRD to prevent air contamination.

***Ab initio* calculation:** All density function theory (DFT) simulations were performed using the Vienna Ab initio Simulation Package (VASP) implementing the pseudopotential plane wave method [15,16]. The Perdew-Burke-Ernzerhof generalized-gradient approximation (PBE-GGA) was used for the exchange–correlation energy [17]. The spin-polarized GGA + U calculations were carried out to account for the correlated d orbitals of TM ions with the Dudarev implementation for the double-counting correction. The effective on-site correlations, $U_{eff} = U - J$ are 4.0 eV, 6.0 eV, 3.1 eV and for Fe, Ni, V respectively [18,19]. A 520 eV plane-wave energy cutoff was used for all calculations.

3. Result and discussion

Fig. 1 shows the XRD patterns of the three as-synthesized $Na_2TM_2F_7$ phases. The main reflections around 29.5° of Fe227 and MgFe227 show mixtures of at least 3 peaks, which is the polymorphism including monoclinic, orthorhombic and trigonal phases in the Weberite phase of $Na_2Fe_2F_7$ [12], while FeVMNT with Fe and V as main elements, and doped with Mg, Ni, and Ti shows weaker polymorphism. Minor impurities include Na_3FeF_6 and Fe_2O_3.

We then ball milled the Fe227 with carbon and assembled it into a Li half-cell with $LiPF_6$ electrolyte and Li metal anode. Fig. 2**a** shows the charge–discharge process of the Fe227 at 0.1C (18 mA/g). During the first charge, about 1Na is de-intercalated from $Na_2Fe_2F_7$ formula, calculated from the measured charge capacity divided by the theoretical capacity for 2Na (de-)intercalation of 184 mAh/g, and diluted to the Li ion electrolyte. During the first discharge, based on the measured discharge capacity of 144 mAh/g, about 1.57Li is inserted into cathode at above 2 V. The first discharge capacity is higher than the charge capacity due to the 1 extra empty Na site in $Na_2Fe_2F_7$, i.e., the fully discharged state is $Na_3Fe_2F_7$. The inset shows the first 3 cycles of this battery. Fig. 2**b** compares the charge–discharge curves of the Fe227 in a Na half-cell ($NaPF_6$ electrolyte and Na metal anode) and the Fe227 in a Li half-cell. Despite the minor differences in shape details, the voltage profile of Li half-cell is similar to that of the Na one. The latter is with Na (de)intercalation in Fe227 [9], with ~ 0.3 V shift down in comparison with the former, due to the voltage difference of the Na and Li metal anodes. The reversible charge–discharge and small voltage polarization (Fig. 2**a**), and the similarity to the Na intercalation voltage curve indicates that the Li intercalation is successfully achieved in Fe227.

Since the crystalline XRD peaks of Fe227 cannot be observed after the ball-milling process, the structural evolution of electrochemical ion exchange in Fig. 2ab cannot be directly measured. Therefore, we use chemical ion exchange to further confirm the Li intercalation chemistry in Fe227. We soak 50 mg Fe227 in 2 ml 5 M LiBr hexanol solution [20] and measure the ex situ XRD over time (Fig. 2**c**). The main peaks of

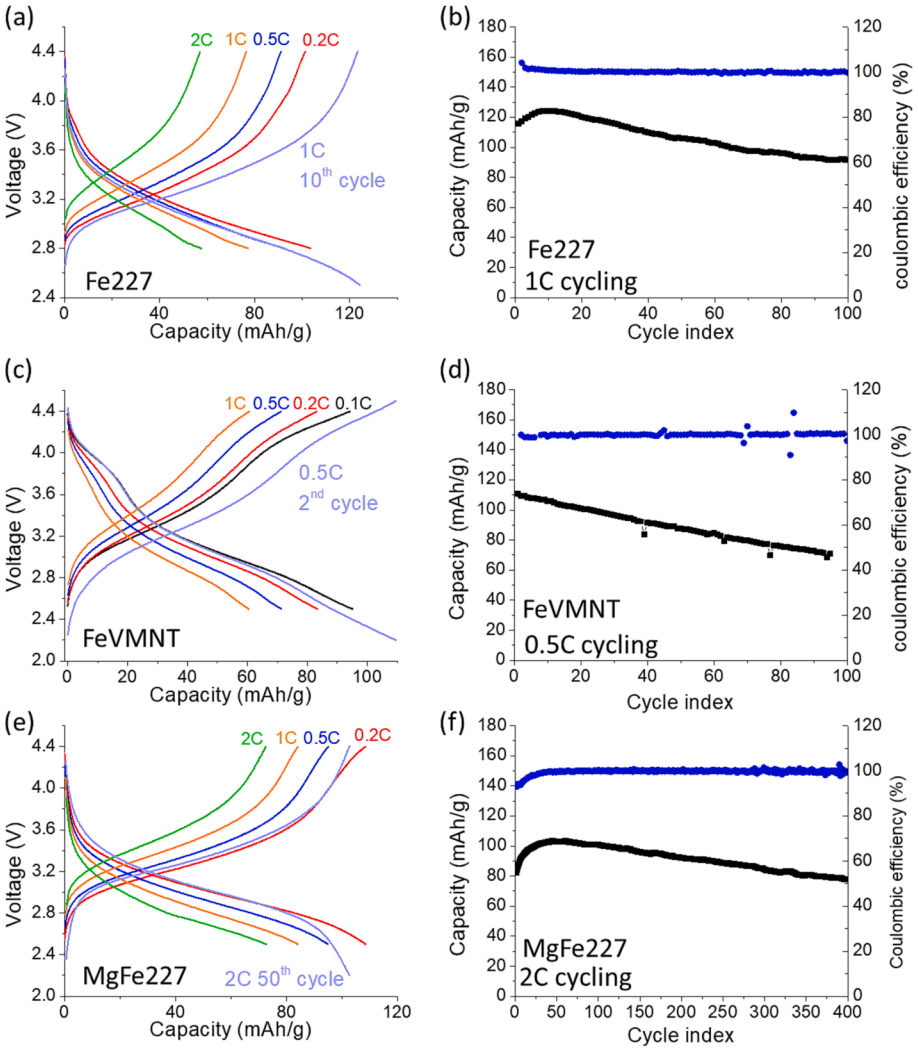

Fig. 3. Voltage curves at different C-rates (a, c, e) and cycling performances (b, d, f) in Li half-cell of (a-b) Fe227, (c-d) FeVMNT and (e-f) MgFe277.

Fe227 shift right over 6 days as labeled by the arrows, suggesting that the overall crystal structure is maintained but the Na ion is gradually replaced by the smaller Li ion. This chemical ion exchange process also shows the opportunity to optimize the Li/Na ratio in the pristine material. However, it is worth noting that a discharge below 2.0 V may incur conversion reactions due to Li insertion beyond the original 3 sites for alkaline ions. Furthermore, considering that there was no report of direct synthesis of $Li_2Fe_2F_7$ or other Li Weberite phases from high temperature sintering, it's likely that Weberite phase favors larger Na ions over smaller Li ions at high temperature, and thus the remaining ≤ 1Na in the formula after the initial charge may also be critical to support the structural stability at room temperature during the battery cycling. This is thus a good example to demonstrate the coupling of synthesis pathways between high temperature sintering through chemical reaction and room temperature synthesis through (electro)chemical (de-) intercalation.

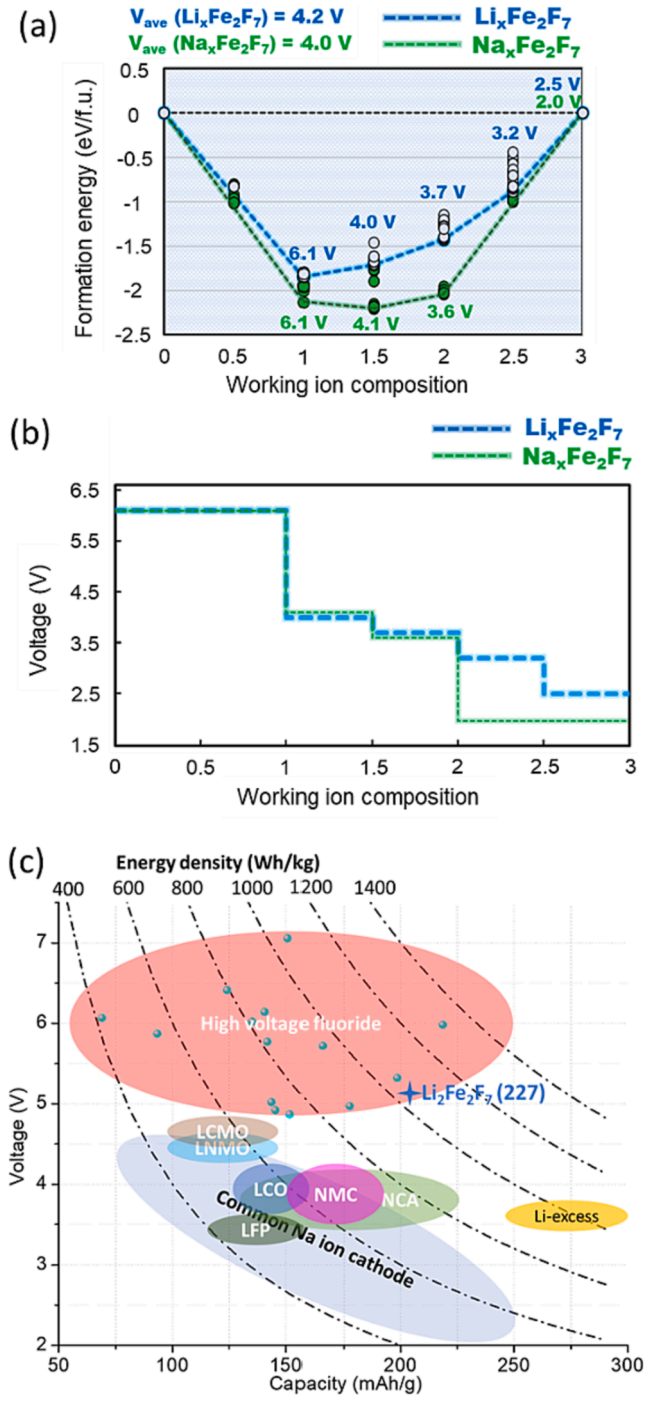

Fig. 4. Computations of cathode performances. (a) Formation energy convex hull of $Li_xFe_2F_7$ and $Na_xFe_2F_7$; (b) Corresponding voltage curves based on the convex hulls; (c) Summary of cathode performances. The $Li_2Fe_2F_7$ point is based on the two Li (de)intercalation of $Fe_2F_7/Li_2Fe_2F_7$.

Fig. 3 shows the electrochemical performance of the three compounds in Li half-cells. Fe227 shows a capacity of 104 mAh/g at 0.2C and 58 mAh/g is maintained at 2C between 2.8 and 4.4 V (Fig. 3**a**). In the cycling test (Fig. 3**b**), Fe227 can cycle in a broader voltage range between 2.5 V and 4.4 V with a maximum capacity of 124 mAh/g at 1C, and the capacity drops to 79 % of the first cycle after 100 cycles.

With other elements doped to Fe227, FeVMNT shows a high voltage plateau at above 3.6 V (Fig. 3**c**). It can cycle at 0.5C with 111 mAh/g between 2.2 V and 4.4 V (Fig. 3**d**). MgFe227 shows a capacity of 108 mAh/g at 0.2C and 72 mAh/g at 2C between 2.4 V – 4.4 V. When enlarging the voltage range to 2.2 V- 4.4 V, MgFe227 can cycle at 2C with a maximum capacity of 103 mAh/g, which drops to 78 mAh/g after 400 cycles. With doping, FeVMNT shows the highest voltage plateau, and $Na_2Mg_{0.5}Fe_{1.5}F_7$ shows the longest cycling stability among the three compounds, demonstrating the opportunity to design new intercalation types of compounds in a broad chemical space. The good cyclability here also indicates that the remaining Na composition in the structure after the initial charge is relatively stable throughout the battery cycling process.

Fig. 4**ab** shows the density functional theory calculation of the voltage curve of $Li_2Fe_2F_7$ and $Na_2Fe_2F_7$. Consistent with literature, $Na_0Fe_2F_7$ to $Na_1Fe_2F_7$ shows a voltage plateau above 6 V [9]. $Li_2Fe_2F_7$ also shows a similar voltage curve in computation, with 0.2 V higher average voltage mainly contributed by the low voltage range. To realize the 6 V capacity in experiment, compatible electrolyte is needed. Our Na/Li ion-exchange strategy also opens the door to a family of intercalation Li metal fluorides that were not accessible previously due to conversion reactions of such compounds from direct chemical synthesis. Fig. 4**c** summarizes cathode material performances, where the family of fluoride cathode materials exhibits the potential to reach beyond 1200 Wh/kg at the cathode material level with high voltage greater than 5 V in our computational prediction. Compared with Li-excess materials with higher capacity and lower voltage, high voltage fluorides will have higher power output and less energy reduction when paired with anode. The full cell design of high cathode loading will also become easier with lower cathode specific capacity at a given energy density.

4. Conclusion

A new type of Li intercalation metal fluoride $Li_xNa_{2-y}TM_2F_7$ is synthesized by solid state reaction and electrochemical ion exchange, which could be a generalizable strategy of combining chemical and electrochemical synthesis pathways at drastically different temperatures to explore the space in the synthesis landscape that is not able to reach by conventional sintering methods. We demonstrate a broad chemical design space by mixing Fe, V, Mg, Ni, Ti, etc. Chemical ion exchange can adjust the Li/Na compositions. Voltage plateau can be tuned by metal doping as demonstrated in $Na_2Mg_{0.2}Ni_{0.1}Ti_{0.1}Fe_{0.8}V_{0.8}F_7$. The compound of $Na_2Mg_{0.5}Fe_{1.5}F_7$ shows a stable cycling of 400 cycles at 2C-rate. This work shows a new design strategy to obtain intercalation type of cathode compounds based on Li metal fluoride from partially ion-exchange with Na ions, which could be crucial to the design of future batteries with significantly enhanced energy density.

CRediT authorship contribution statement

Yichao Wang: Methodology, Investigation, Writing – original draft. **Xianguang Miao:** Methodology, Investigation. **Yitong Li:** Methodology, Investigation. **Hwanyeol Park:** Methodology, Investigation. **Yang Lu:** Methodology. **Xin Li:** Conceptualization, Supervision, , Funding

acquisition, Investigation, Methodology, Project administration, Resources, Writing – review & editing ..

Declaration of Competing Interest

The authors declare that they have no known competing financial interests or personal relationships that could have appeared to influence the work reported in this paper.

Data availability

Data will be made available on request.

Acknowledgments

The work is supported by Johnson Matthey and Harvard Climate Change Solutions Fund. The computation is supported by Extreme Science and Engineering Discovery Environment (XSEDE) Stampede and Frontera clusters.

References

[1] K. Turcheniuk, D. Bondarev, G.G. Amatucci, G. Yushin, Battery materials for low-cost electric transportation, Mater. Today 42 (2021) 57–72.
[2] H. Li, P. Balaya, J. Maier, Li-storage via heterogeneous reaction in selected binary metal fluorides and oxides, J. Electrochem. Soc. 151 (2004) A1878.
[3] N. Twu, X. Li, C. Moore, G. Ceder, Synthesis and lithiation mechanisms of dirutile and rutile LiMnF4: two new conversion cathode materials, J. Electrochem. Soc. 160 (2013) A1944.
[4] F. Wu, V. Srot, S. Chen, S. Lorger, P.A. van Aken, J. Maier, Y. Yu, 3D honeycomb architecture enables a high-rate and long-life iron (III) fluoride–lithium battery, Adv. Mater. 31 (2019) 1905146.
[5] L. Sun, Y. Li, W. Feng, Metal fluoride cathode materials for lithium rechargeable batteries: focus on iron fluorides, Small Methods 7 (2023) 2201152.
[6] C. Li, K. Chen, X. Zhou, J. Maier, Electrochemically driven conversion reaction in fluoride electrodes for energy storage devices, npj Comput. Mater. 4 (2018) 22.
[7] X. Wang, W. Gu, J.T. Lee, N. Nitta, J. Benson, A. Magasinski, M.W. Schauer, G. Yushin, Carbon Nanotube–CoF2 Multifunctional Cathode for Lithium Ion Batteries: Effect of Electrolyte on Cycle Stability, Small 11 (2015) 5164–5173.
[8] D. Andre, H. Hain, P. Lamp, F. Maglia, B. Stiaszny, Future high-energy density anode materials from an automotive application perspective, J. Mater. Chem. A 5 (2017) 17174–17198.
[9] H. Park, Y. Lee, M.-K. Cho, J. Kang, W. Ko, Y.H. Jung, T.-Y. Jeon, J. Hong, H. Kim, S.-T. Myung, J. Kim, Na2Fe2F7: a fluoride-based cathode for high power and long life Na-ion batteries, Energy Environ. Sci. 14 (2021) 1469–1479.
[10] J. Liao, J. Han, J. Xu, Y. Du, Y. Sun, L. Duan, X. Zhou, Scalable synthesis of Na 2 MVF 7 (M= Mn, Fe, and Co) as high-performance cathode materials for sodium-ion batteries, Chem. Commun. 57 (2021) 11497–11500.
[11] J. Kang, J. Ahn, H. Park, W. Ko, Y. Lee, S. Lee, S. Lee, S.-K. Jung, J. Kim, Highly Stable Fe2+/Ti3+-Based Fluoride Cathode Enabling Low-Cost and High-Performance Na-Ion Batteries, Adv. Funct. Mater. 32 (2022) 2201816.
[12] E.E. Foley, V.C. Wu, W. Jin, W. Cui, E. Yoshida, A. Manche, R.J. Clément, Polymorphism in Weberite Na2Fe2F7 and its Effects on Electrochemical Properties as a Na-Ion Cathode, Chem. Mater. 35 (2023) 3614–3627.
[13] U.K. Dey, N. Barman, S. Ghosh, S. Sarkar, S.C. Peter, P. Senguttuvan, Topochemical Bottom-Up Synthesis of 2D- and 3D-Sodium Iron Fluoride Frameworks, Chem. Mater. 31 (2019) 295–299.
[14] O. Yakubovich, V. Urusov, W. Massa, G. Frenzen, D. Babel, Structure of Na2Fe2F7 and structural relations in the family of weberites Na2MIIMIIIF7, Z. Anorg. Allg. Chem. 619 (1993) 1909–1919.
[15] G. Kresse, G. Kresse and J. Furthmüller, Phys. Rev. B 54, 11169 (1996), Phys. Rev. B, 54 (1996) 11169.
[16] G. Kresse, G. Kresse and J. Furthmüller, Comput. Mater. Sci. 6, 15 (1996), Comput. Mater. Sci., 6 (1996) 15.
[17] J.P. Perdew, JP Perdew, K. Burke, and M. Ernzerhof, Phys. Rev. Lett. 77, 3865 (1996), Phys. Rev. Lett., 77 (1996) 3865.
[18] G. Hautier, S.P. Ong, A. Jain, C.J. Moore, G. Ceder, Accuracy of density functional theory in predicting formation energies of ternary oxides from binary oxides and its implication on phase stability, Phys. Rev. B 85 (2012), 155208.
[19] Y. Nanba, T. Iwao, B.M.d. Boisse, W. Zhao, E. Hosono, D. Asakura, H. Niwa, H. Kiuchi, J. Miyawaki, Y. Harada, M. Okubo, A. Yamada, Redox Potential Paradox in NaxMO2for Sodium-Ion Battery Cathodes, Chem. Mater., 28 (2016) 1058-1065.
[20] J. Paulsen, C. Thomas, J. Dahn, Layered Li-Mn-oxide with the O2 structure: a cathode material for Li-ion cells which does not convert to spinel, J. Electrochem. Soc. 146 (1999) 3560.